Supporting Information (SI)

Ni Doping in $CsPbCl_3$ Nanocrystals: The Key to Enhanced Photoluminescence

Soumya Panja,[a] Prasenjit Mandal,[a] Subhashri Mannar,[b] Arpan Das,[c] Shobhana Narasimhan,[c] Ranjani Viswanatha [a,b]*

[a]New Chemistry Unit, [b] International Centre for Material Science, [c] Theoretical Sciences Unit, Jawaharlal Nehru Centre for Advanced Scientific Research, Jakkur, Bangalore 560064, India.

*Corresponding Author

*Email: rv@jncasr.ac.in

Tables:

Figures:

S13: Temperature dependent FWHM curve of steady state band-edge emission with fitting for Ni-doped NCs.

S14: Steady state PL spectra of physical mixture of undoped and doped NCs with C-30 dye.

S15: Lifetime decay curve of physical mixture of undoped NCs with C-30 dye.

1. Experimental methods:

Synthesis of the undoped and Ni-doped perovskites was carried out by following the earlier reported colloidal synthesis method with slight modification.[1,2]

Chemicals:

Chemicals used for synthesis purposes including cesium carbonate (Cs_2CO_3, Sigma Aldrich, 99.99%), lead(II) chloride ($PbCl_2$, 99.999%), lead(II) acetate trihydrate ($Pb(CH_3COO)_2 \cdot 3H_2O$, 99.99%), nickel(II) chloride ($NiCl_2$, 99.999%), nickel(II) acetate tetrahydrate ($Ni(CH_3COO)_2 \cdot 4H_2O$, 99.99%), benzoyl chloride (C_6H_5COCl, 98%), 1-octadecene (ODE, technical grade, 90%), oleylamine (OLAm, 70%), oleic acid (OA, 90%), n-hexane (> 97%), methyl acetate (CH_3COOCH_3) and coumarin-30 ($C_{21}H_{21}N_3O_2$) were purchased from Sigma-Aldrich. All solvents and reagents were of analytical grade and directly used after purchase without any further purification.

Preparation of cesium oleate (Cs-Oleate):

400 mg Cs_2CO_3 were added into a 50 ml 3-necked round bottom (RB) flask along with 1.5 ml OA and 20 ml ODE and degassed for 1hr at 120° C. Then purged argon (Ar) into the flask and heated up to 150° C until Cs_2CO_3 fully dissolved in the solution to form Cs-Oleate. After that, it was cooled to room temperature using a water bath and stored in a degassed glass

vial. It must be preheated at 100° C before use since at room temperature Cs-Oleate precipitates out of ODE.

Synthesis of undoped and Ni-doped $CsPbCl_3$ by cation injection method:

For undoped $CsPbCl_3$, 0.188 mmol $PbCl_2$, 1 ml OA, 1ml OLAm, and 5 ml ODE were added in a 50 ml RB followed by degassing for 1 hr at 120° C. Then purged Ar into it and increased the temperature to 180° C and inject previously prepared 0.4 ml Cs-Oleate and quenched it immediately using an ice-water bath. A similar procedure was followed for the synthesis of Ni-doped $CsPbCl_3$, only the required amount of $NiCl_2$ was added depending upon the Pb:Ni stoichiometric ratio along with 0.188 mmol $PbCl_2$, 1 ml OA, 1 ml OLAm, and 5 ml ODE in 50 ml RB flask. Ni incorporation requires first breaking the existing strong Pb-Cl bond before the formation of Ni-Cl bond in this method.

Synthesis of undoped and Ni-doped $CsPbCl_3$ by anion injection method:

In a 50 ml RB flask 0.05 mmol Cs_2CO_3, 0.2 mmol $Pb(CH_3COO)_2{\cdot}3H_2O$, 1 ml OA, 1 ml OLAm, and 5 ml ODE were loaded and dried under vacuum for 1 hr at 120° C. Subsequently increased the temperature to 180° C under Ar atmosphere. Then at 180° C 1.8 mmol of benzoyl chloride was injected and quenched immediately using an ice-water bath. The synthesis of Ni-doped $CsPbCl_3$ followed the similar procedure, where the appropriate quantity of $Ni(CH_3COO)_2{\cdot}4H_2O$ was added based on the Pb:Ni stoichiometric ratio. This was carried out along with the addition of 0.05 mmol Cs_2CO_3, 0.2 mmol $Pb(CH_3COO)_2{\cdot}3H_2O$, 1 ml OA, 1 ml OLAm, and 5 ml ODE in a 50 ml RB flask. Here, Pb-Cl and Ni-Cl bonds form simultaneously, leading to higher Ni incorporation efficiency.

Isolation and purification:

The resulting mixture was precipitated by centrifugation at 5000 rpm for 10 minutes. After centrifugation supernatant was discarded and dried the precipitation properly. The resulting precipitation was redispersed in hexane and stored in refrigerator for further characterization.

Washing procedure:

After synthesizing undoped and Ni-doped $CsPbCl_3$ we washed the sample with an appropriate sample to antisolvent methyl acetate (CH_3COOCH_3) ratio and centrifuged it. After centrifugation, we collected the precipitation and dissolved in hexane for further characterization.

2. Characterization and spectroscopic techniques:

Synthesized nanocrystals (NCs) were characterized and studied through different structural and optical characterization techniques.

Perkin Elmer Avio 550 max inductively coupled plasma optical emission spectrometer has been used to obtain the elemental percentages present inside the NCs. Elemental analysis was carried out with samples dissolved in a mixture of HNO_3 and HCl with 1:3 ratio. The Ni and Pb concentrations were measured against known standards of high purity purchased from Sigma-Aldrich to determine the actual percentage of Ni-doping.

Crystal structure identification of the particles was carried out using X-ray diffraction (XRD) recorded on Rigaku advance diffractometer using Cu-K_α radiation having wavelength 1.5406 Å. Since the diffracted intensities from these NCs are generally weak, all patterns were recorded at a slow scan rate with 2θ ranges from 10° to 60° in order to get high signal-to-noise

ratio. The bulk reference XRD pattern collected from the inorganic crystal structure database (ICSD).

Extended X-ray absorption fine structure spectroscopy (EXAFS) was carried out at the synchrotron facility PETRA-III of DESY, a member of the Helmholtz Association (HGF), Germany. The samples are dropcasted on scotch tapes and the measurements were done in reflection geometry in fluorescence mode. For the host Pb L_{III}-edge and dopant Ni K-edge we have calibrated the incident X-ray energy to 13035.2 eV and 8332.8 eV respectively. The collected data are processed in Athena software and fitting is done with Artemis software, part of the Demeter package. Through calibrating the respective edge energy several scan data are merged to get better quality data before fitting with theoretical standards.

X-band electron spin resonance spectroscopy (ESR) has been done using JEOL JES-X320 instrument with the highest magnetic field 1.3 T. Measurements are done using quartz capillary at room temperature.

The size and morphology of NCs were studied out using transmission electron microscopy (TEM). TEM was carried out in JEOL JEM-2100 plus transmission electron microscope using lanthanum hexaboride (LaB_6) electron gun with an accelerating voltage of 200 kV. Samples for TEM were prepared by adding a drop of NCs solution dissolved in hexane on carbon coated pure Cu-200 grid. The solvent was allowed to evaporate leaving behind the NCs for imaging.

High-angle annular dark field - scanning transmission electron microscopy with energy dispersive X-ray spectroscopy (HAADF-STEM EDX) performed in JEOL JEM-F200 with cold field electron gun having an accelerating voltage of 200 kV in STEM mode.

Ultraviolet-visible (UV-Vis) absorption spectra of both undoped and Ni-doped $CsPbCl_3$ perovskite NCs dissolved in hexane were obtained using Agilent 8453 UV-visible spectrometer using quartz cuvette.

Magnetic circular dichroism (MCD) spectra are collected from Oxford S065633 MCD instrument. Measurements are done by mounting samples in variable temperature insert (2 – 20 K) with 0 – 5 T superconducting magnet. The probe light from the xenon lamp (50 W) was modulated between left and right circularly polarized light and allowed to pass through the sample. The amount of transmitted light was detected using a photomultiplier tube detector.

Steady state photoluminescence (PL) spectra were collected using xenon lamp as the source on the FLS-1000 Edinburgh spectrometer, while the gated PL with different delay time and lifetime measurements were carried out in the same instrument using micro-seconds flash lamp as an excitation source (E_{ex} = 3.4 eV). Gated PL measurement with a 50 μs gating time implies that the sample is excited at t = 0 seconds, and the emission spectra are collected starting at t = 50 μs. Low temperature measurements were done using cryostat with liquid helium cooling. NCs films were cooled down to 10 K and measurements were done at every 20 K interval while increasing temperature up to 295 K. For power-dependent time-resolved PL (TRPL) measurements, we used 340 nm light-emitting diode (LED) source with a maximum power of 1.2 μW.

3. Computational details:

DFT calculations were performed using the Quantum ESPRESSO software package.[3] The Kohn-Sham wavefunctions and the corresponding charge densities were expanded in plane-wave basis sets having cutoffs of 45 Ry and 450 Ry respectively. Exchange-correlation interactions were treated using the Perdew-Burke-Ernzerhof form of the Generalized Gradient

Approximation (PBE-GGA).[4] The interactions between valence electrons and ionic cores were described using ultrasoft pseudopotentials.[5] We have considered the cubic unit cell of $CsPbCl_3$, made a 2×2×2 supercell in which one Pb atom was substituted by one Ni atom to make a 12.5% Ni-doped system. All the cell parameters and atomic coordinates were relaxed using the Broyden-Fletcher-Goldfarb-Shanno (BFGS) algorithm until all components of the forces on all atoms were less than 0.001 Ry/Bohr. The Brillouin zone sampling was done using a 4 × 4 × 4 Monkhorst-Pack k-point mesh[6] and Marzari-Vanderbilt cold smearing[7] of width 0.005 Ry was used to improve convergence.

4. Tables and figures:

Table S1. Sample code and actual doping percentage table of undoped and Ni-doped synthesized samples obtained from elemental analysis using ICP-OES.

Sample	Pb:Ni (molar ratio)	Synthesis method	Pb (%)	Ni (%)
P1	1:0	Cation injection	100.00	0.00
$Ni_{0.5}$P1	1:0.25	Cation injection	99.53 ± 0.06 ≈ 99.50	0.47 ± 0.06 ≈ 0.50
Ni_1P1	1:0.02	Anion injection	98.97 ± 0.03 ≈ 99.00	1.03 ± 0.03 ≈ 1.00
Ni_2P1	1:1	Cation injection	98.12 ± 0.08 ≈ 98.00	1.88 ± 0.08 ≈ 2.00
Ni_3P1	1:0.05	Anion injection	96.80 ± 0.04 ≈ 97.00	3.20 ± 0.04 ≈ 3.00

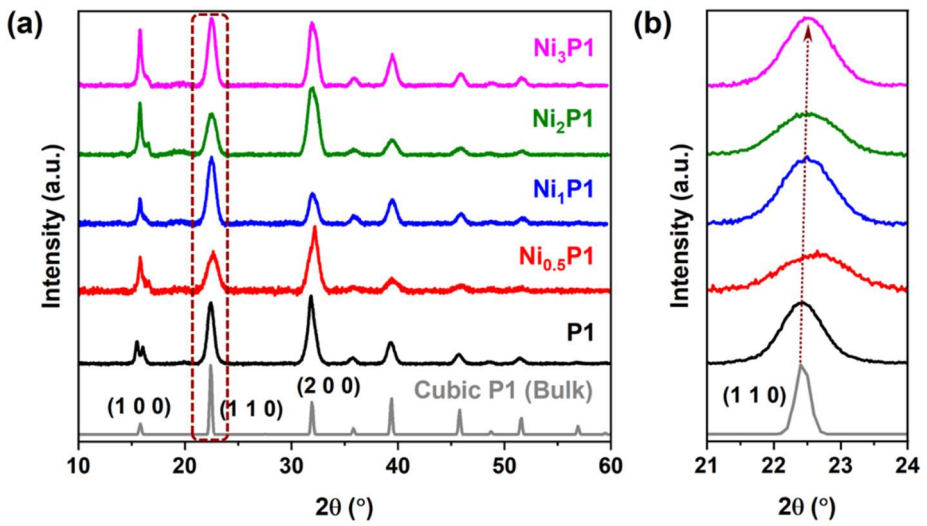

Figure S1. (a) XRD pattern for full 2θ range; (b) magnified view of the XRD peak corresponding to (110) plane of undoped and all Ni-doped NCs with bulk reference data.

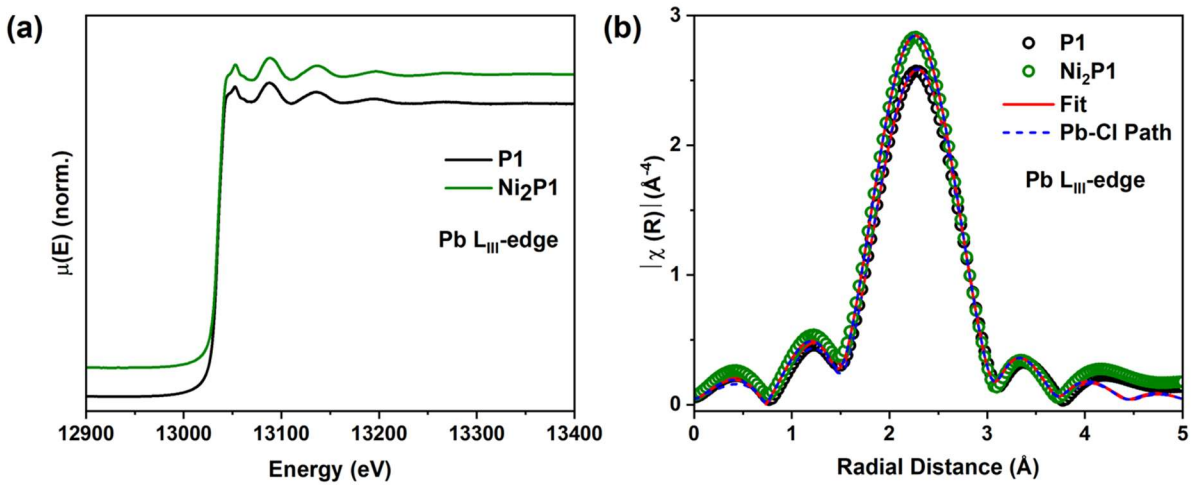

Figure S2. Pb L_{III}-edge (a) typical EXAFS spectra as a function of incident photoelectron energy; (b) k^3-weighted magnitude of Fourier-transformed EXAFS spectra (hollow circle) along with best fit (red solid line) and the possible theoretical path for fitting (blue dashed line) of undoped (P1) and 2% (Ni_2P1) Ni-doped $CsPbCl_3$ NCs. [Here, μ(E): absorption coefficient as a function of incident photoelectron energy (E) and χ(R): XAFS oscillations as a function of radial distance (R) from the absorbing atoms.]

Table S2. List of fitting parameters [number of independent points (N_{ind}), number of variables (N_{var}), coordination number (CN), energy shift (ΔE_0), Debye-Waller factor (σ^2), bond length (R), and R-factor] obtained from the best fit for host Pb L_{III}-edge as well as dopant Ni K-edge for both undoped and doped NCs.

Sample	Paths	CN	ΔE_0 (eV)	σ^2 (Å^{-2})	R (Å)	R-factor
P1 **Pb L_{III}-edge** *k*: 3 – 7.5 Å^{-1} R: 1 – 4.5 Å N_{ind}: 12 N_{var}: 4	Pb−Cl	5.4 ± 0.3	0.58 ± 0.54	0.016 ± 0.001	2.85 ± 0.01	0.002
Ni_2P1 **Pb L_{III}-edge** *k*: 3 – 7.5 Å^{-1} R: 1 – 4.5 Å N_{ind}: 10 N_{var}: 4	Pb−Cl	6.0 ± 0.4	-0.71 ± 0.59	0.016 ± 0.001	2.84 ± 0.01	0.004
Ni_2P1 **Ni K-edge** *k*: 2.2 – 6 Å^{-1} R: 1 – 4 Å N_{ind}: 7 N_{var}: 3	Ni−Cl Ni−Z_{low}	5.76 1	0.6 -0.02	0.029 ± 0.003 0.005	2.67 ± 0.01 2.12 ± 0.02	0.027

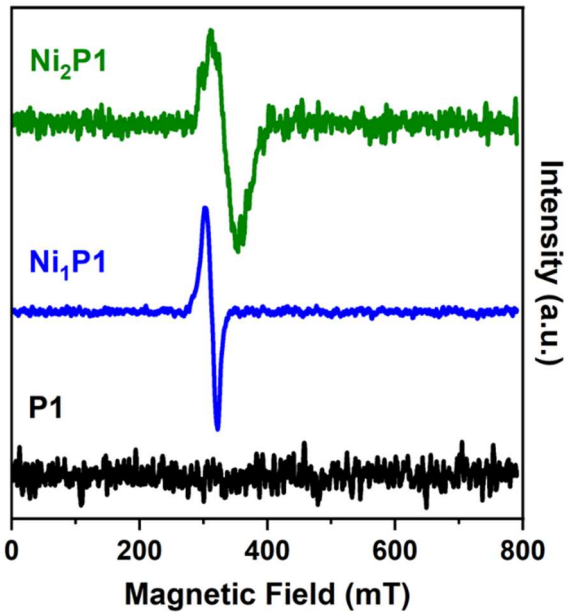

Figure S3. Room temperature ESR spectra of undoped (P1) and Ni-doped $CsPbCl_3$ (Ni_xP1; x = 1, 2) NCs

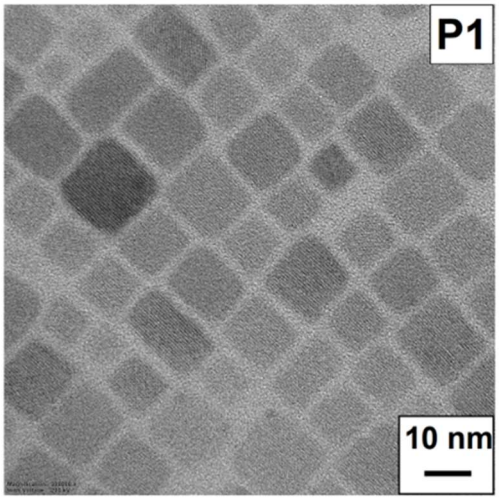

Figure S4. TEM image of undoped $CsPbCl_3$ (P1) NCs.

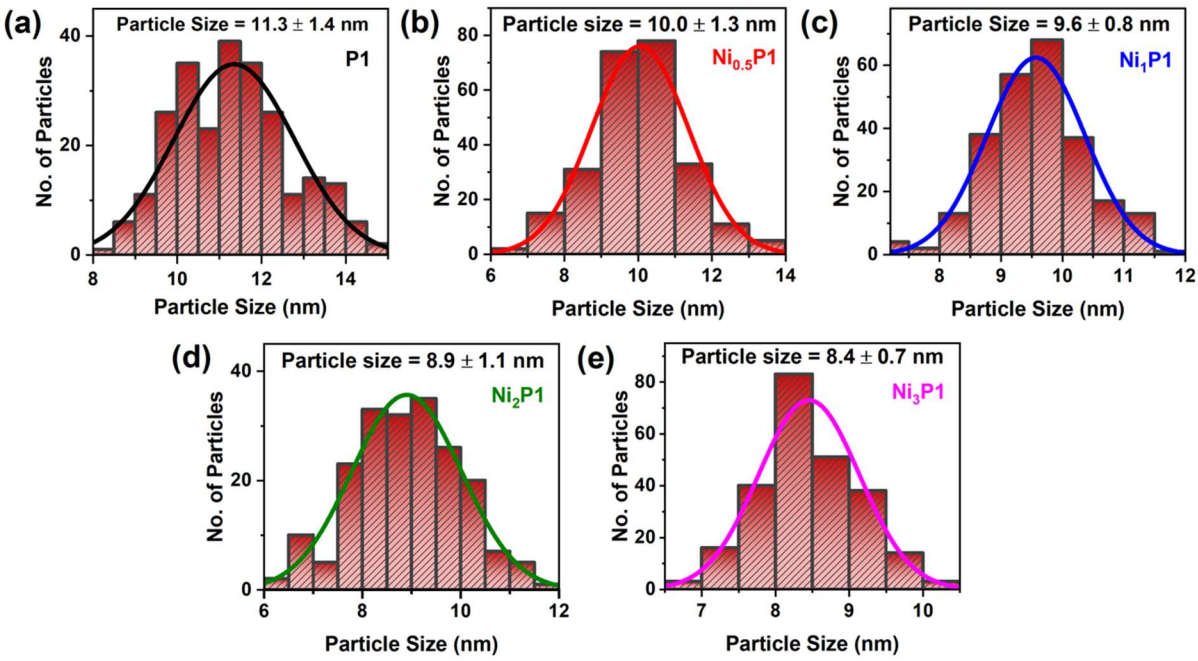

Figure S5. Particle size histograms of (a) undoped (P1); (b) 0.5% ($Ni_{0.5}P1$); (c) 1% (Ni_1P1) (d) 2% (Ni_2P1) and (e) 3% (Ni_3P1) Ni-doped $CsPbCl_3$.

Table S3. Average particle size analysis of undoped and various Ni-doped $CsPbCl_3$.

Sample	Ni (%)	Particle size (nm)
P1	0.0	11.3 ± 1.4
$Ni_{0.5}P1$	0.5	10.0 ± 1.3
Ni_1P1	1.0	9.6 ± 0.8
Ni_2P1	2.0	8.9 ± 1.1
Ni_3P1	3.0	8.4 ± 0.7

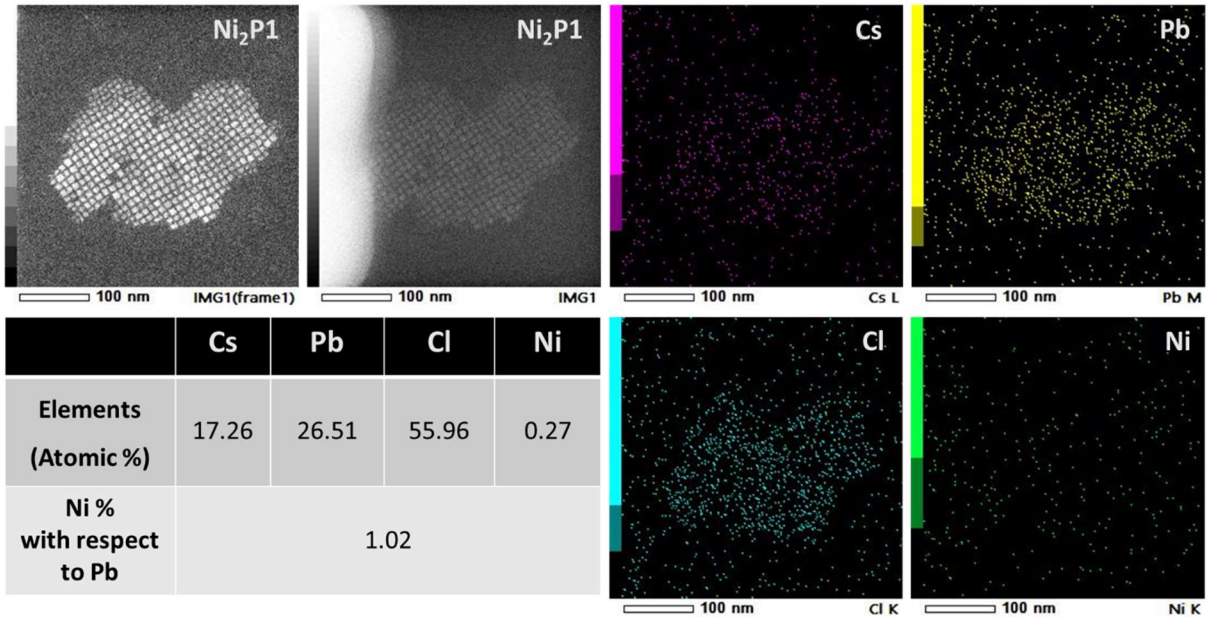

	Cs	Pb	Cl	Ni
Elements (Atomic %)	17.26	26.51	55.96	0.27
Ni % with respect to Pb	1.02			

Figure S6. HAADF-STEM EDX elemental mapping of 2% Ni-doped $CsPbCl_3$ (Ni_2P1) NCs with 100 nm resolution and the corresponding Ni percentage with respect to Pb.

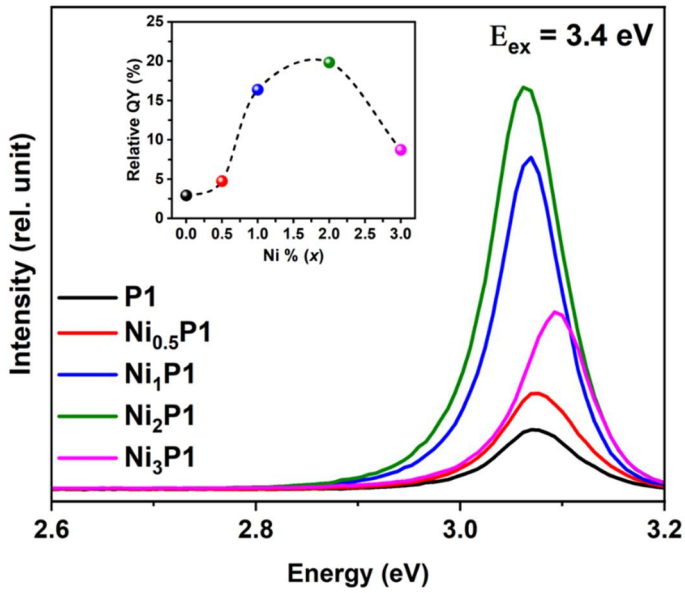

Figure S7. Steady state PL intensity for undoped (P1) and various Ni-doped $CsPbCl_3$ (Ni_xP1; x = 0.5, 1, 2, 3) at room temperature (E_{ex} = 3.4 eV) along with inset of relative QY variation with doping percentages.

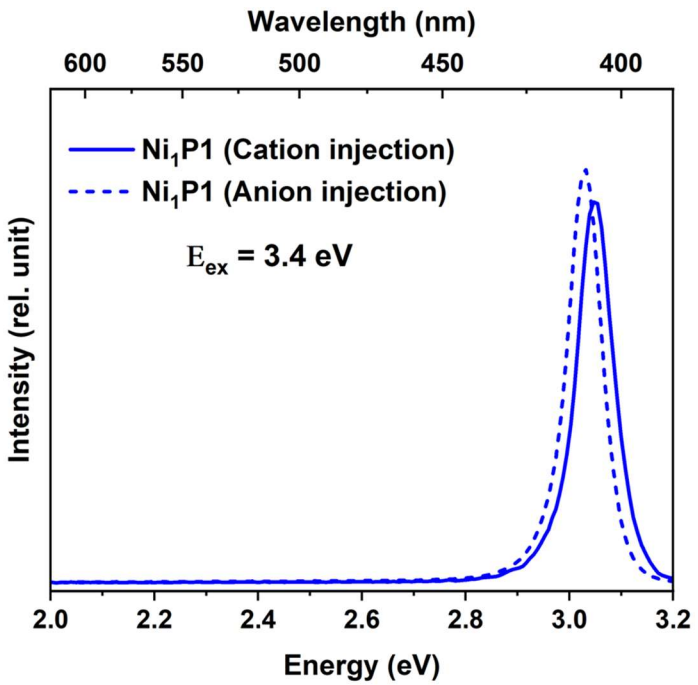

Figure S8. Steady state PL intensity for 1% Ni-doped $CsPbCl_3$ (Ni_1P1) synthesized via different methods cation and anion injection (E_{ex} = 3.4 eV).

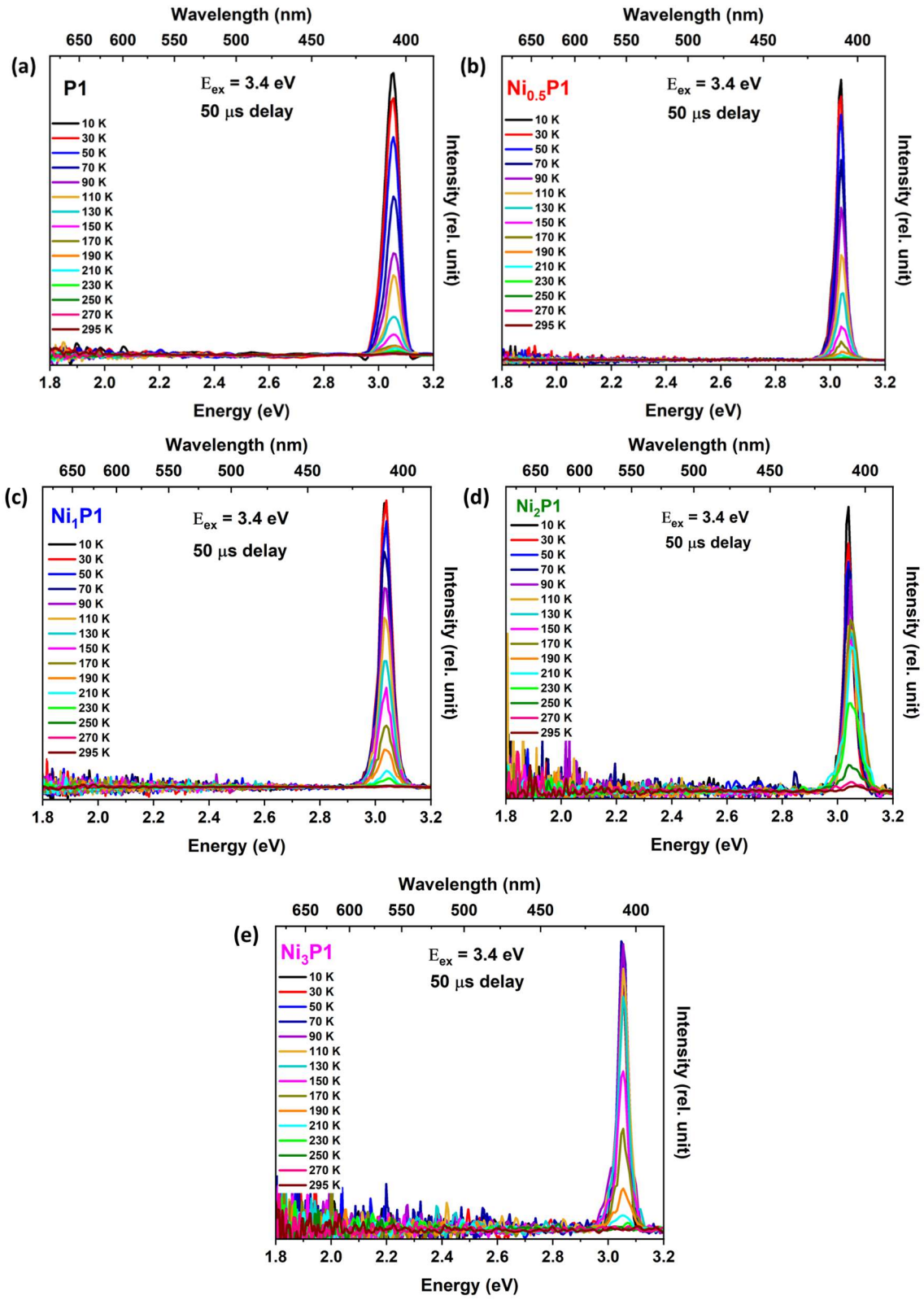

Figure S9. Temperature dependent gated PL with 50 μs gating time of (a) undoped (P1); (b) 0.5% ($Ni_{0.5}P1$); (c) 1% (Ni_1P1); (d) 2% (Ni_2P1) and (e) 3% (Ni_3P1) Ni-doped $CsPbCl_3$.

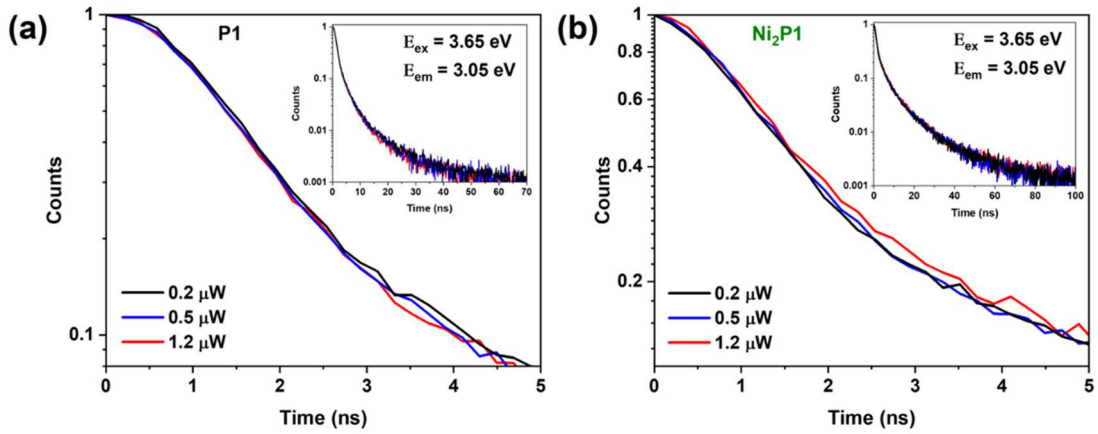

Figure S10. Power-dependent TRPL decay curve of (a) undoped (P1) and (b) 2% Ni-doped (Ni_2P1) $CsPbCl_3$ NCs with an inset showing the lifetime decay curve in full timescale.

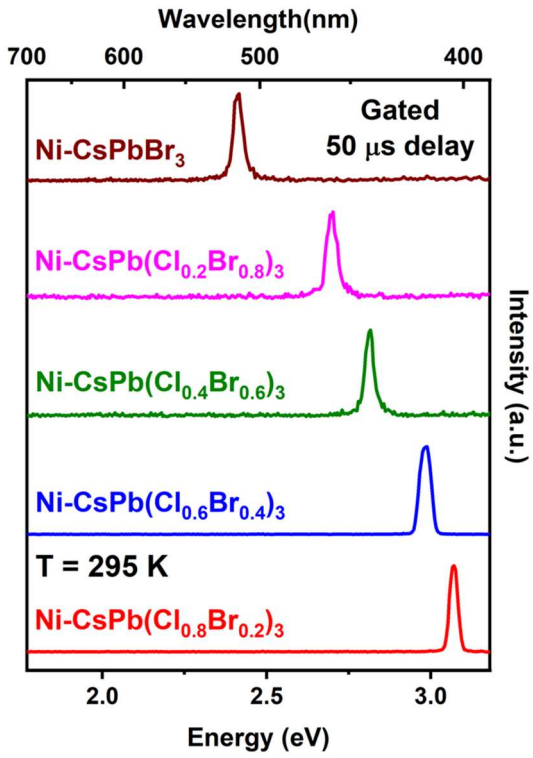

Figure S11. Gated excitonic emission with 50 μs gating time for Ni-doped mixed halide $CsPb(Cl_yBr_{1-y})_3$ perovskites at 295 K.

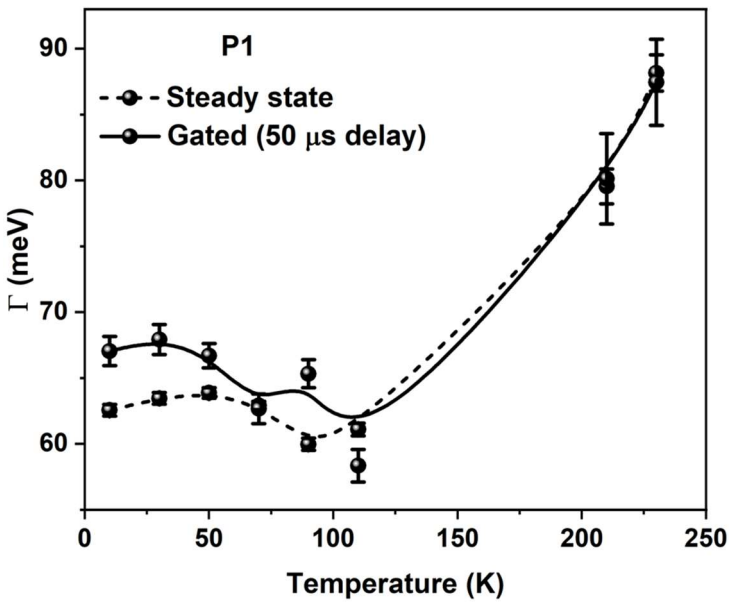

Figure S12. Temperature dependent FWHM (Γ) curve of steady state as well as gated PL excitonic emission of undoped $CsPbCl_3$ (P1).

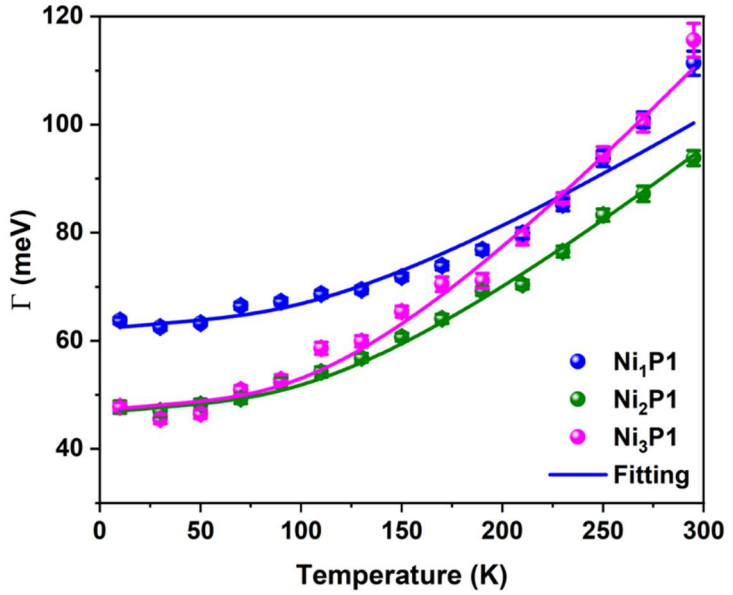

Figure S13. Temperature dependent FWHM curve for steady state PL excitonic emission along with fitting by equation $\Gamma(T) = \Gamma_0 + \gamma_{ac}T + \frac{\gamma_{lo}}{(e^{\frac{E_{lo}}{k_B T}} - 1)}$ for Ni-doped NCs.

Table S4. Fitting parameters [FWHM at T = 0 K (Γ_0), coupling strength of exciton with acoustic phonon (γ_{ac}) and longitudinal optical phonon (γ_{lo}) and longitudinal optical phonon energy (E_{lo})] obtained from the fitting of temperature dependent FWHM in steady state PL emission for Ni-doped NCs by equation $\Gamma(T) = \Gamma_0 + \gamma_{ac}T + \frac{\gamma_{lo}}{(e^{\frac{E_{lo}}{k_B T}} - 1)}$.

Sample	Ni %	Γ_0 (meV)	γ_{ac} (μeV/K)	γ_{lo}(meV)	E_{lo} (meV)
Ni_1P1	1	62.2 ± 0.5	33 ± 7	87.55 ± 13.67	13.67 ± 1.00
Ni_2P1	2	46.7 ± 0.7	33 ± 7	117.08 ± 19.18	13.67 ± 1.00
Ni_3P1	3	47.1 ± 0.6	33 ± 7	165.20 ± 29.56	13.67 ± 1.00

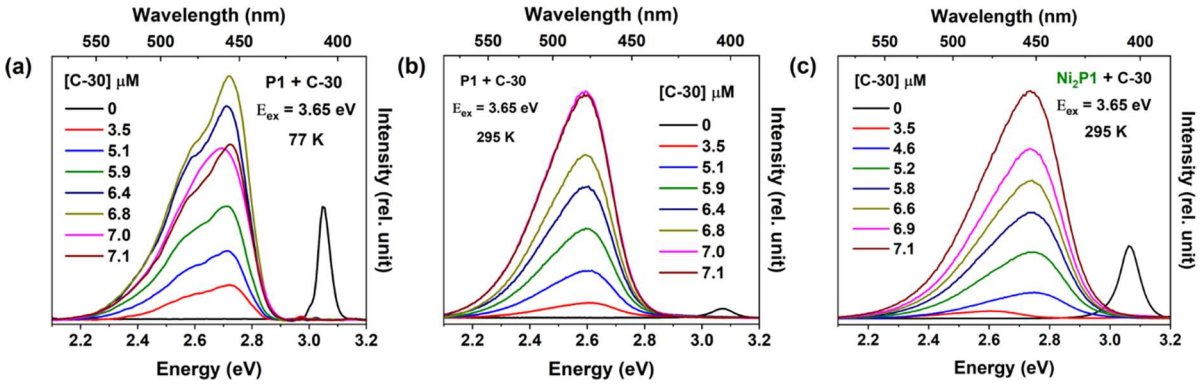

Figure S14. Steady state PL of undoped (P1) and C-30 physical mixture at (a)77 K and (b) 295 K; (c) 2% Ni-doped $CsPbCl_3$ (Ni_2P1) and C-30 physical mixture at 295 K.

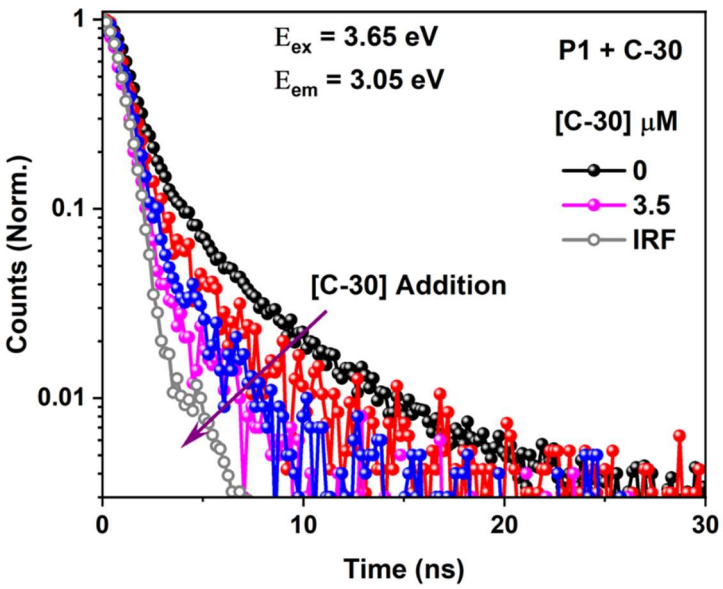

Figure S15. Lifetime decay curve of physical mixture of undoped and C-30 dye with varying dye concentration.

References:

1 L. Protesescu, S. Yakunin, M. I. Bodnarchuk, F. Krieg, R. Caputo, C. H. Hendon, R. X. Yang, A. Walsh and M. V. Kovalenko, *Nano Lett.*, 2015, **15**, 3692–3696.

2 M. Imran, V. Caligiuri, M. Wang, L. Goldoni, M. Prato, R. Krahne, L. De Trizio and L. Manna, *J. Am. Chem. Soc.*, 2018, **140**, 2656–2664.

3 P. Giannozzi, S. Baroni, N. Bonini, M. Calandra, R. Car, C. Cavazzoni, D. Ceresoli, G. L. Chiarotti, M. Cococcioni, I. Dabo, A. Dal Corso, S. de Gironcoli, S. Fabris, G. Fratesi, R. Gebauer, U. Gerstmann, C. Gougoussis, A. Kokalj, M. Lazzeri, L. Martin-Samos, N. Marzari, F. Mauri, R. Mazzarello, S. Paolini, A. Pasquarello, L. Paulatto, C. Sbraccia, S. Scandolo, G. Sclauzero, A. P. Seitsonen, A. Smogunov, P. Umari and R. M.

Wentzcovitch, *J. Phys. Condens. Matter*, 2009, **21**, 395502.

4 J. P. Perdew, K. Burke and M. Ernzerhof, *Phys. Rev. Lett.*, 1996, **77**, 3865–3868.

5 D. Vanderbilt, *Phys. Rev. B*, 1990, **41**, 7892–7895.

6 H. J. Monkhorst and J. D. Pack, *Phys. Rev. B*, 1976, **13**, 5188–5192.

7 N. Marzari, D. Vanderbilt, A. De Vita and M. C. Payne, *Phys. Rev. Lett.*, 1999, **82**, 3296–3299.